

**SUPPLEMENTARY INFORMATION**

**Eco-friendly Synthesis of Porous Reduced Graphene Oxide-Polypyrrole-Gold Nanoparticles Hybrid Nanocomposite for Electrochemical Detection and Monitoring of Methotrexate Using a Strip Sensor**

Reshmi A Sukumaran<sup>a</sup>, Kavitha Lakavath<sup>a</sup>, Phani Kumar V. V. N. <sup>b</sup>, Sampath Karingula<sup>a</sup>, Kuldeep Mahato<sup>c</sup>, Yugender Goud Kotagiri\*<sup>a</sup>

<sup>a</sup> *Department of Chemistry, Indian Institute of Technology Palakkad, Palakkad, Kerala 678 557, India*

<sup>b</sup> *Centre for Automotive Energy Materials, International Advanced Research Centre for Powder Metallurgy and New Materials (ARCI), Chennai 600113, Tamil Nadu, India.*

<sup>c</sup> *Department of NanoEngineering, University of California San Diego, 9500 Gilman Drive, La Jolla, California 92093, United States*

*Corresponding Authors Details*

*Dr. Yugender Goud Kotagiri*

*Assistant Professor,*

*Department of Chemistry,*

*Indian Institute of Technology Palakkad,*

*Palakkad, Kerala 678 557, India.*

*E-mail: [yugenderkotagiri@iitpkd.ac.in](mailto:yugenderkotagiri@iitpkd.ac.in)*

## SUPPLEMENTARY INFORMATION

### Contents

1. Chemicals and Materials.....	3
2. Preparation of Graphene Oxide.....	3
3. SPCE cleaning process.....	3
4. Fabrication of the PrGO–PPy–Au Modified Screen-Printed Sensor.....	4
5. TGA .....	5
6. SEM.....	6
7. EDAX .....	7
8. UV .....	7
9. IR analysis .....	8
10. BET and DFT of PrGO-PPy-Au.....	8
11. BJH .....	8
12. Randles equivalent circuit.....	9
13. Cyclic Voltammograms of Different scan rate .....	10
14. Electrochemically Active Surface Area (ECSA) of BARE electrode .....	11
15. Electrochemically Active Surface Area (ECSA) of the drop-casted electrode .....	12
16. Transducer Layer Optimization.....	13
17. pH optimization .....	14
18. Selectivity.....	14
19. Comparison Table .....	15
20. The detection limit (LOD) was calculated using the 3-sigma method .....	15
21 Instrumentation .....	16
22. References .....	17

## SUPPLEMENTARY INFORMATION

### **1. Chemicals and Materials**

Methotrexate 99.8% purity were procured from TCI, Japan. Graphite powder (crystalline 99%) and 5-Fluorouracil was purchased from TCI Chemicals. Sulfuric acid ( $\text{H}_2\text{SO}_4$ , 99.9%), sodium nitrate ( $\text{NaNO}_3$ , 99%), potassium permanganate ( $\text{KMnO}_4$ , 99%), hydrogen peroxide ( $\text{H}_2\text{O}_2$  30% w/w in  $\text{H}_2\text{O}$ ), hydrochloric acid ( $\text{HCl}$  37%) were purchased from Sigma-Aldrich, India. Ethanol, gold (III) chloride hydrate ( $\text{HAuCl}_4$ ), Potassium chloride, ferricyanide  $[\text{Fe}(\text{CN})_6]^{4-}$ , sodium hydroxide ( $\text{NaOH}$ ), dopamine(DA), L-Ascorbic acid (AA), Folic acid(FA) and uric acid (UA), Pyrrole, Sodium borohydride were purchased from SRL Chemicals India. All of the ordered chemicals were of analytical grade standard 90–99%. Phosphate-buffered saline (PBS) solution electrolyte materials (AR-grade, 99%), potassium chloride ( $\text{KCl}$ ). 98% human serum (Sigma-Aldrich), All the mentioned chemicals were used for analysis without any further purifications.

### **2. Preparation of Graphene Oxide**

Graphene oxide (GO) was synthesized from graphite powder using a simplified version of the Hummers method. The process included these steps: 1.5 grams of graphite powder was pre-oxidized with 20 ml of concentrated sulfuric acid ( $\text{H}_2\text{SO}_4$ ) and 0.75 grams of sodium nitrate ( $\text{NaNO}_3$ ). The mixture was stirred in cold conditions for at least 4 hours. Then, 4.5 grams of potassium permanganate ( $\text{KMnO}_4$ ) was added and stirred for at least 1 hour while keeping it cold. The temperature was then increased to  $50^\circ\text{C}$ , and the mixture was stirred for 4 hours. Afterward, 50 ml of distilled water was added, and the temperature was raised to  $90^\circ\text{C}$  and maintained for 1 hour. Next, a mixture of 100 ml double-distilled water and 12.5 ml of 30% hydrogen peroxide ( $\text{H}_2\text{O}_2$ ) was added, causing the solution to turn brownish. Continuous stirring was maintained for 1 hour. Finally, the solution was centrifuged and repeatedly washed with 5% hydrochloric acid ( $\text{HCl}$ ) and double-distilled water. The solid GO was then dried for further use<sup>1</sup>.

### **3. SPCE cleaning process**

A spotless and dust-free SPCE substrate is essential for the effective immobilization of nanomaterials. To achieve this, the electrode underwent an electrochemical pretreatment process prior to SPCE modification. This process involved applying multiple potential cycles between 1.0 and -1.5 V versus the  $\text{Ag}/\text{AgCl}$  reference electrode at a scan rate of 100 mV/s in

## SUPPLEMENTARY INFORMATION

a solution of 0.5 M H<sub>2</sub>SO<sub>4</sub> and 0.1 M KCl. The process was continued until a distinctive voltammogram of a clean SPCE surface was achieved. This activation of the bare SPCE electrode surface improves interactions between the SPCE and the immobilized nanotubes, which is a critical step in preparing the electrode for electrochemical measurements.

### **4. Fabrication of the PrGO–PPy–Au Modified Screen-Printed Sensor.**

The PrGO-PPy-Au was applied to the SPCE surface through a straightforward drop-casting method. Initially, the SPCEs underwent thorough cleaning with ethanol and water. The PrGO-PPy-Au nanocomposite was subsequently prepared by mixing the synthesized black powder with chitosan and sonicating the mixture for 30 minutes to produce a uniform ink solution. To optimize the nanocomposite loading, this ink was applied to the SPCE surface using drop-casting in different volumes (1, 2, 3, and 4 μL). Following drop-casting, the electrodes were left to air-dry at room temperature for 12 hours. These electrodes, referred to as SPCE/PrGO-PPy-Au, were then used as transducers for electrochemical sensing. To improve selectivity and antifouling characteristics, a thin Nafion layer was coated onto the electrodes, yielding the final version labeled SPCE/PrGO-PPy-Au/Nafion. Nafion, a perfluorinated polymer, efficiently blocks the adsorption of interfering substances on the electrode surface.

CV is a robust method for examining electrochemical systems, offering comprehensive insights into the reactions occurring at the electrode surface. In this study, CV was employed with K<sub>3</sub>[Fe(CN)<sub>6</sub>] to investigate the improved electron transfer on a modified SPCE featuring a graphene-Au nanocomposite within a conducting polymer. The measurements were conducted in a 2 mM K<sub>3</sub>[Fe(CN)<sub>6</sub>] solution with 0.1 M KCl buffer, using a scan rate of 100 mV/s. Electrochemical impedance spectroscopy (EIS) is commonly used to explore the interfacial properties of electrochemical systems. In this study, EIS was performed with a 2 mM K<sub>3</sub>[Fe(CN)<sub>6</sub>] redox probe in a 0.1 M KCl aqueous solution. Measurements were recorded at open-circuit potential over a frequency range from 100 kHz to 10 mHz, with data collected at a rate of 12 points per decade. A 30-second quiet time was allowed before each measurement to ensure stability and accuracy. SWV & CA are widely used methods for studying reaction kinetics mechanisms. SWV provides benefits over CV, including quicker analysis, higher sensitivity, and a wider dynamic range. For SWV, measurements were

## SUPPLEMENTARY INFORMATION

carried out with a potential range of 0.4 to 1 V, a frequency of 10 Hz, a step potential of 10 mV, and an amplitude of 50 mV. Meanwhile, CA measurements were taken at 0.76 V relative to Ag/AgCl for a duration of 60 seconds.

In this study, both SWV and CA techniques were utilized to detect and analyze MTX at low concentrations in PBS buffer and real human serum. The modified SPCE sensor was employed for MTX detection in human serum sourced from Sigma-Aldrich, without additional processing, and showcased outstanding performance with exceptional sensitivity and selectivity.

### 5. TGA

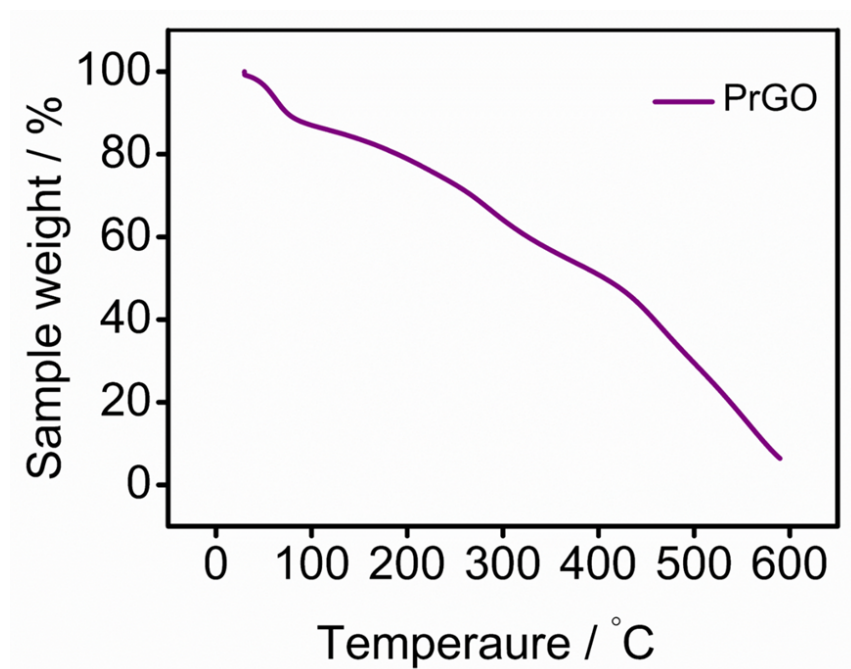


**Fig. S1.** Thermogravimetric analysis (TGA) curves of PrGO

### 6. SEM

**SUPPLEMENTARY INFORMATION**

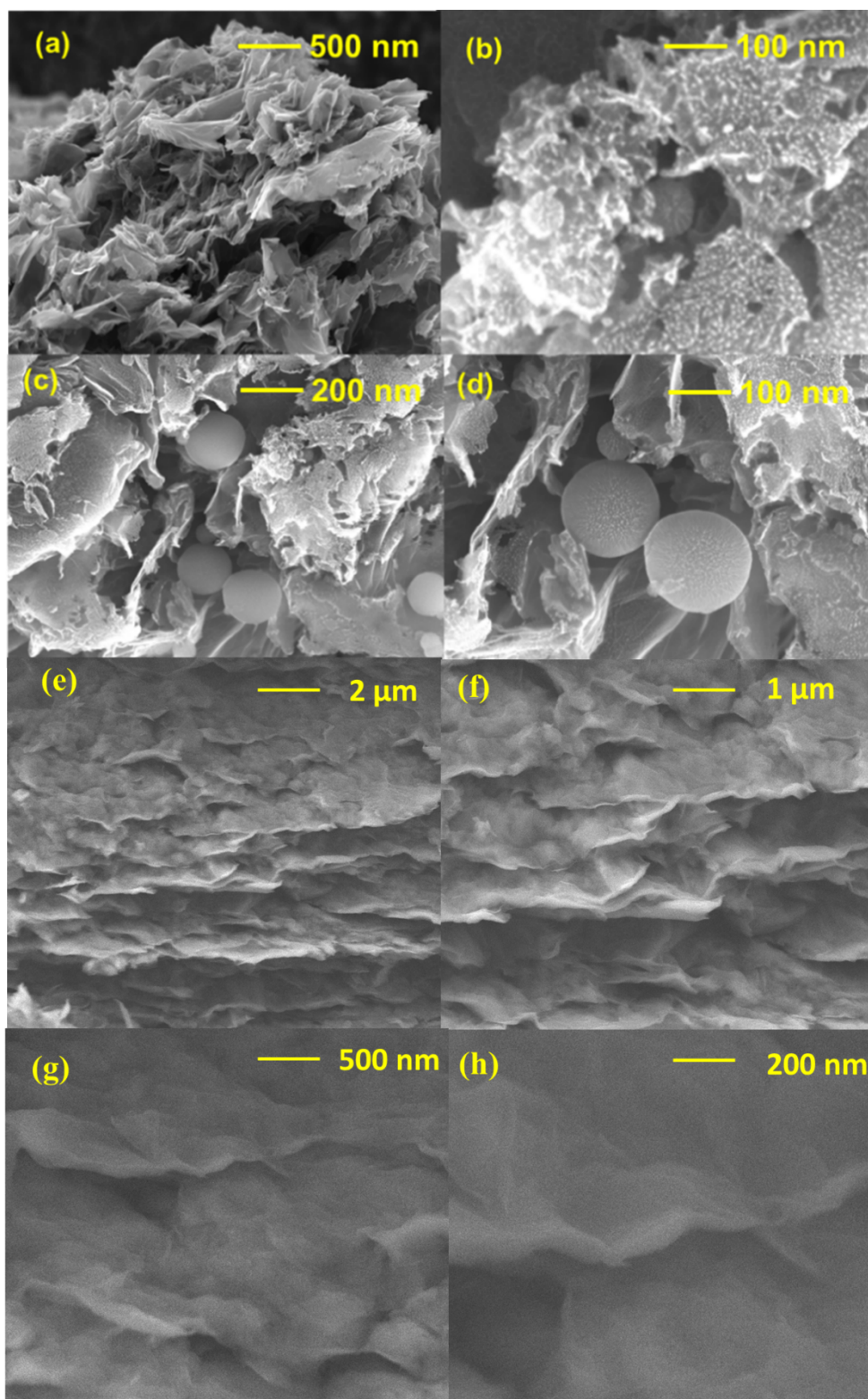


**Fig. S2.** SEM images of PrGO at (a) 500 nm resolution and (b) 100 nm resolution; SEM images of PrGO-PPy at (c) 200 nm resolution and (d) 100 nm resolution. SEM images of GO at (e) 2 μm resolution and (f) 1 μm resolution (g) 500 nm resolution and (h) 200 nm resolution.

## SUPPLEMENTARY INFORMATION

### 7. EDAX

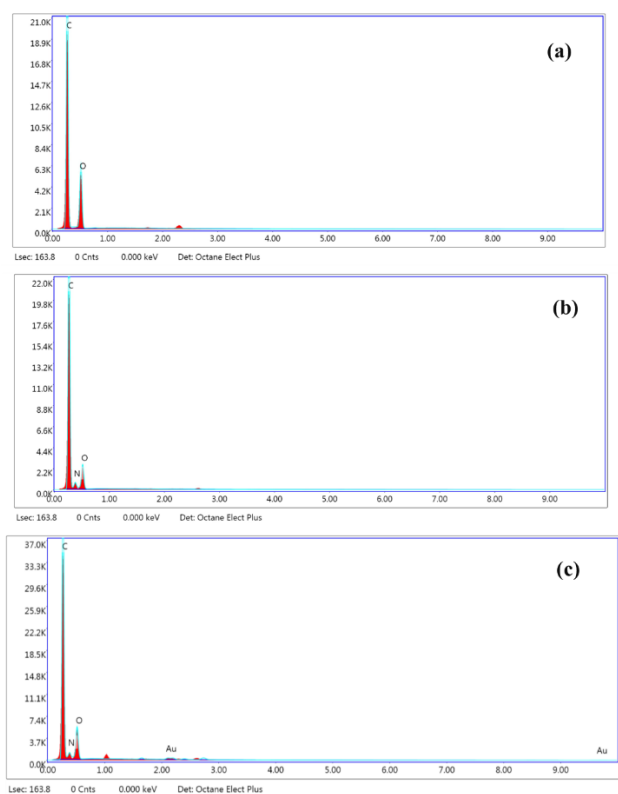


**Fig. S3.** EDX spectrum of the (a) PrGO, (b) PrGO-PPy and (c) PrGO-PPy-Au nanocomposite.

### 8. UV

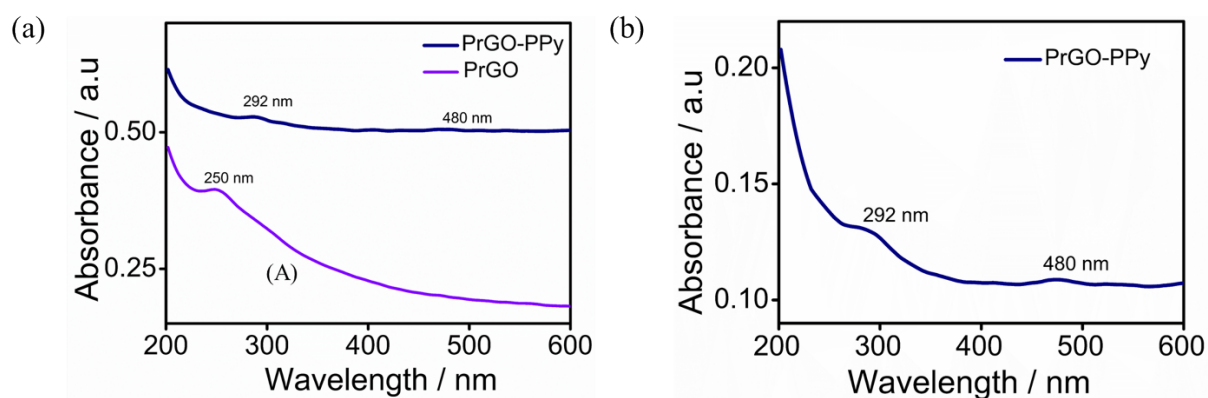


**Fig. S4.** (a) UV comparison of PrGO and PrGO-PPy. (b) UV spectrum of PrGO-PPy.

### 9. IR analysis

## SUPPLEMENTARY INFORMATION

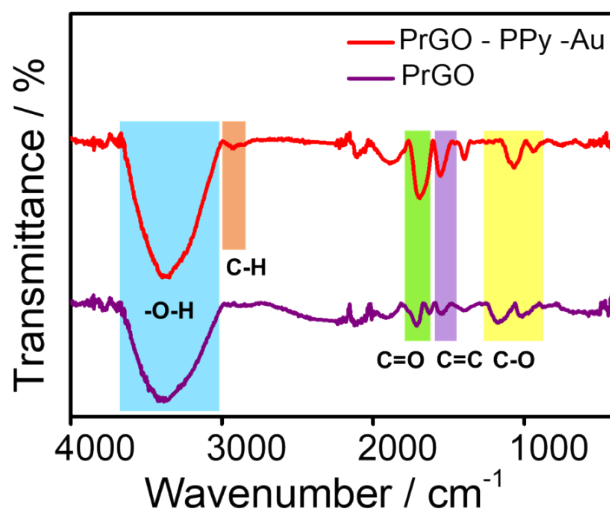


Fig. S5. FTIR spectrum of PrGO and PrGO-PPy-Au.

### 10. BET and DFT of PrGO-PPy-Au

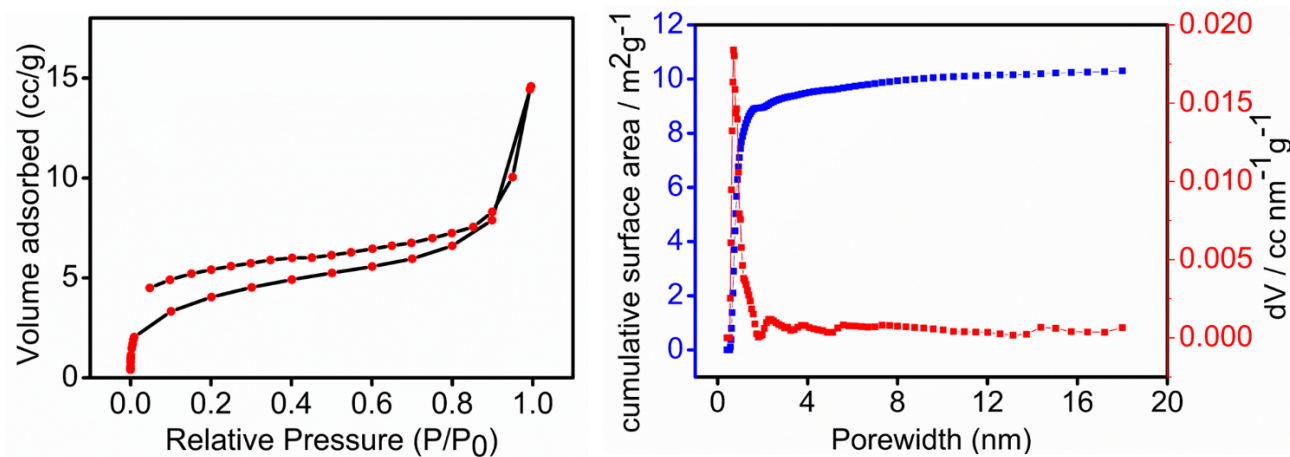


Fig. S6. Surface Area and Pore Size Characterization (a) adsorption/desorption isotherm, and (b) DFT pore distribution of PrGO-PPy-Au (This pattern of adsorption isotherm closely resembles the adsorption behavior previously reported for microporous polymer materials<sup>2</sup>)

### 11. BJH



## SUPPLEMENTARY INFORMATION

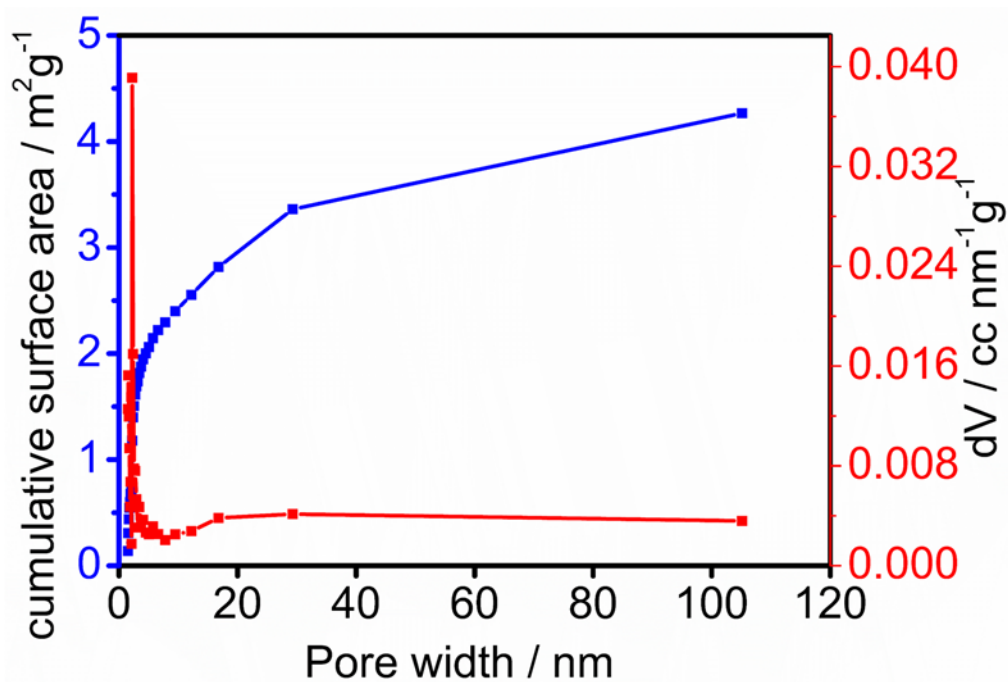
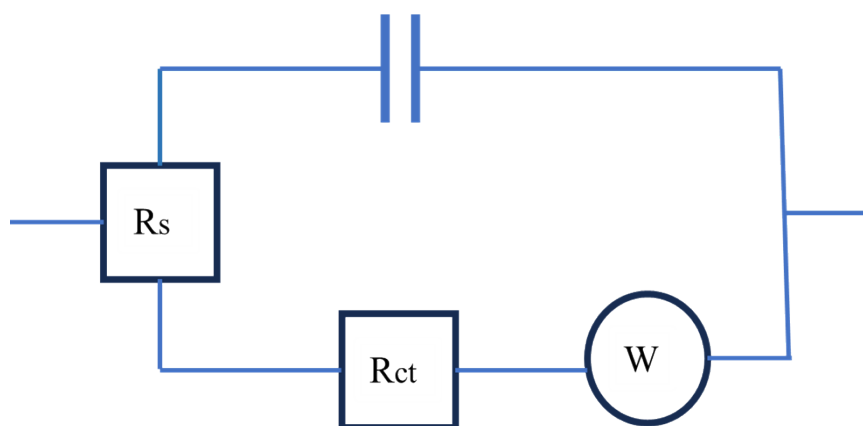


Fig. S7. BJH pore-size distribution of PrGO

## 12. Randles equivalent circuit



$R_s$  - Solution Resistance

$R_{ct}$  - Charge Transfer Resistance

$W$  - Warburg Impedance

## SUPPLEMENTARY INFORMATION

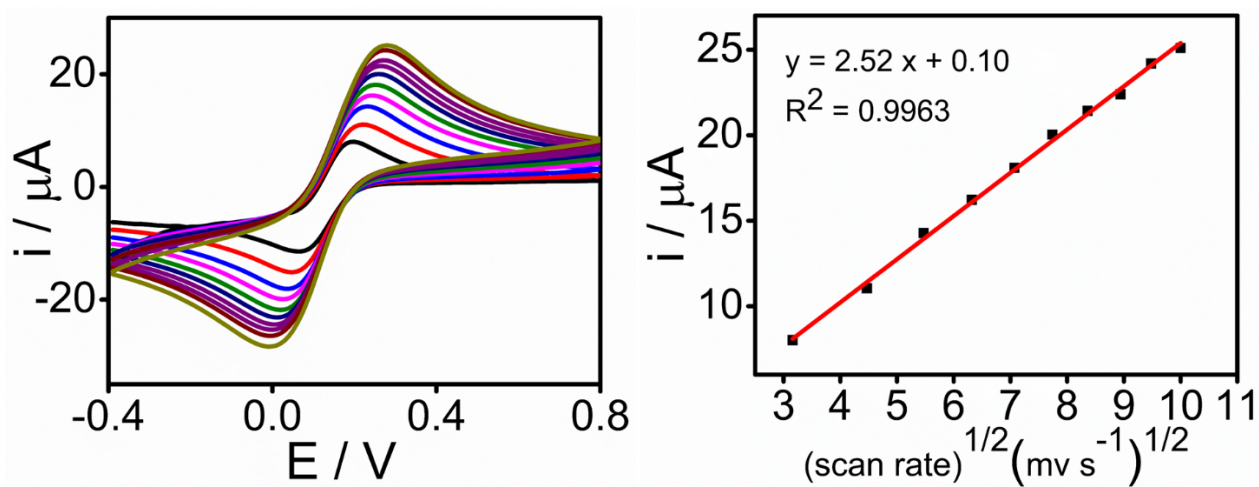
|| - Capacitor

**Fig. S8.** Schematic representation of Randles equivalent circuit

**Table S1.** Charge transfer resistance values of the bare and modified electrodes.

S.NO	Electrode	Charge transfer resistance ( $R_{ct}$ ) in $\Omega$
1.	SPCE	1133
2.	PrGO	650
3.	PrGO – PPy	244
4.	PrGO – PPy -Au	132

### 13. Cyclic Voltammograms of Different scan rate



## SUPPLEMENTARY INFORMATION

**Fig. S9.** (A) Effect of scan rate (10-100 mV/s) on cyclic voltammetry in 2 mM  $K_3[Fe(CN)_6]$  + 0.1 M KCl solution on bare electrode vs Ag/AgCl. (B) Plot of anodic peak currents ( $i_{pa}$ ) vs. scan rate

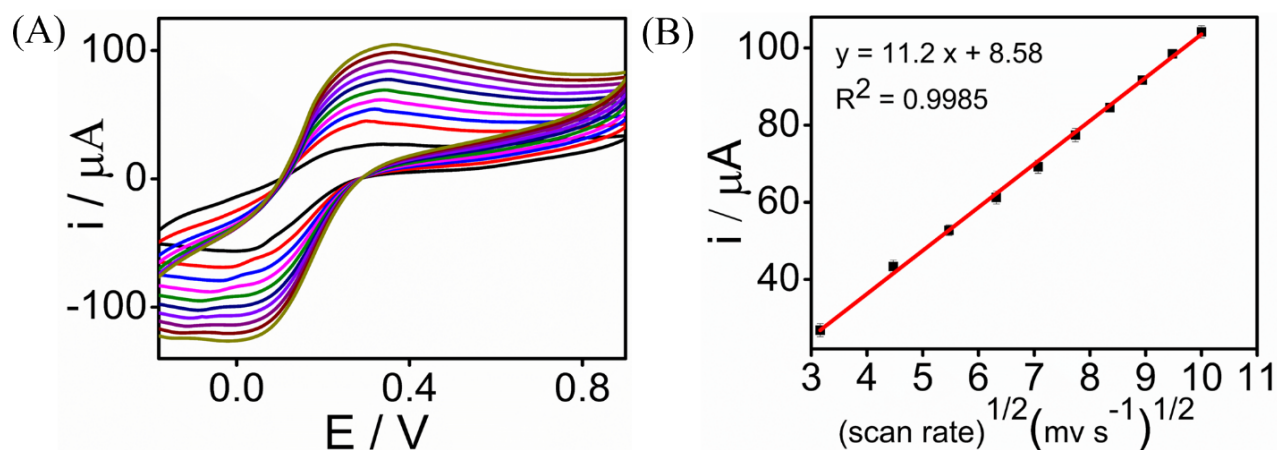


**Fig. S10.** (A) Effect of scan rate (10-100 mV/s) on cyclic voltammetry of rGO/PPy-Au/Chi in 2 mM  $K_3[Fe(CN)_6]$  + 0.1 M KCl solution vs Ag/AgCl. (B) Plot of anodic peak currents ( $i_{pa}$ ) vs. scan rate.

### 14. Electrochemically Active Surface Area (ECSA) of BARE electrode

Calculation of Electrochemically Active Surface Area Values (Randles-Sevcik Equation)

$$I = 2.69 \times 10^5 \times n^{3/2} \times A \times D \times C \times v^{1/2}$$

The observed slope values from the graph of  $I$  vs  $v^{1/2}$  for bare electrode

$$y = 2.52x + 0.10$$

From here, Slope,  $m = 2.52$

*Electrochemically active surface area* = Slope value from the graph  $\times 3.16228 \times 10^{-5} /$

$$2.69 \times 10^5 \times n^{3/2} \times \sqrt{D} \times C$$

*Electrochemically active surface area* =

$$2.52 \times 3.16228 \times 10^{-5} / 2.69 \times 10^5 \times 1^{3/2} \times \sqrt{6.7 \times 10^{-6}} \times 5 \times 10^{-6}$$

## SUPPLEMENTARY INFORMATION

$$= 2.52 \times 3.1628 \times 10^{-5} / 13.923 \times 10^{-4}$$

$$= 0.0572$$

***Electrochemically active surface area of bare electrode = 0.0572***

### **15. Electrochemically Active Surface Area (ECSA) of the drop-casted electrode**

Calculation of Electrochemically Active Surface Area Values (Randles-Sevcik Equation)

$$I = 2.69 \times 10^5 \times n^{3/2} \times A \times D^{1/2} \times C \times v^{1/2}$$

The observed slope values from the graph of I vs  $v^{1/2}$  for AuNPs-PPy-PrGO is

$$y = 11.52 x + 8.58$$

From here, Slope,  $m = 11.52$

*Electrochemically active surface area = Slope value from the graph  $\times 3.16228 \times 10^{-5} /$*

$$2.69 \times 10^5 \times n^{3/2} \times \sqrt{D} \times C$$

*Electrochemically active surface area =*

$$11.52 \times 3.16228 \times 10^{-5} / 2.69 \times 10^5 \times 1^{3/2} \times \sqrt{6.7 \times 10^{-6}} \times 5 \times 10^{-6}$$

$$= 11.52 \times 3.1628 \times 10^{-5} / 13.923 \times 10^{-4}$$

$$= 0.261$$

***Electrochemically active surface area of the drop-casted electrode = 0.261***

**Sensitivity = Slope of the calibration curve / ECSA (From SWV in PBS)**

$$= 1.59 / 0.261$$

$$= 6.09 \mu\text{A}/\mu\text{M}/\text{cm}^2$$

**Sensitivity = Slope of the calibration curve / ECSA (From SWV in Serum)**

$$= 6.311 / 0.261$$

## SUPPLEMENTARY INFORMATION

$$= 24.1 \mu\text{A}/\mu\text{M}/\text{cm}^2$$

Sensitivity = Slope of the calibration curve / ECSA (From CA in Serum)

$$= 0.003/0.261$$

$$= 0.011 \mu\text{A}/\text{nM}/\text{cm}^2$$

$$= 11 \mu\text{A}/\mu\text{M}/\text{cm}^2$$

### 16. Transducer Layer Optimization

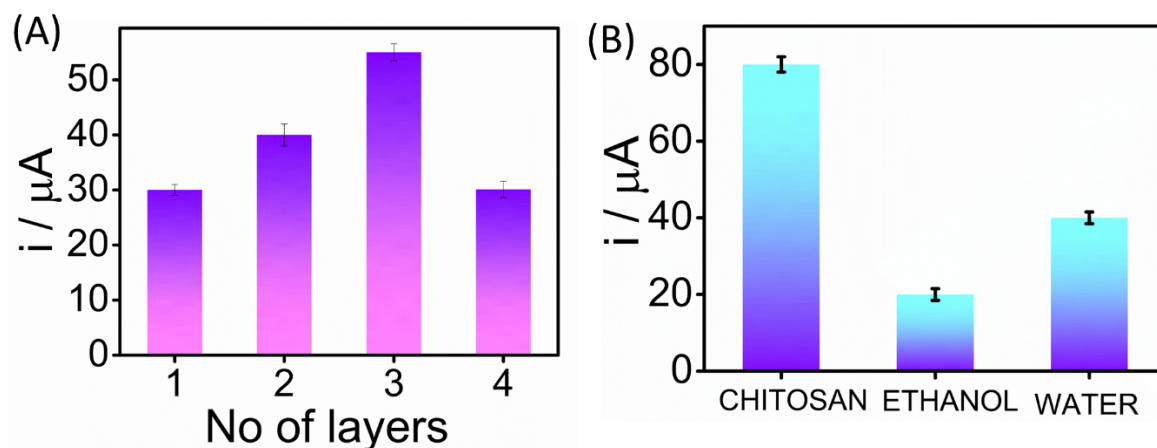


**Fig. S11.** (A) Cyclic voltammogram response of different layer modifications of SPCE with PrGO-Ppy-Au in 2 mM Ferri-ferro cyanide. (B) Optimization of PrGO-Ppy-Au dissolved in chitosan, ethanol, and water, with current values obtained from cyclic voltammetry at a potential range of -0.2 V to 0.9 V and a scan rate of 100 mV/s.

### 17. pH optimization

## SUPPLEMENTARY INFORMATION

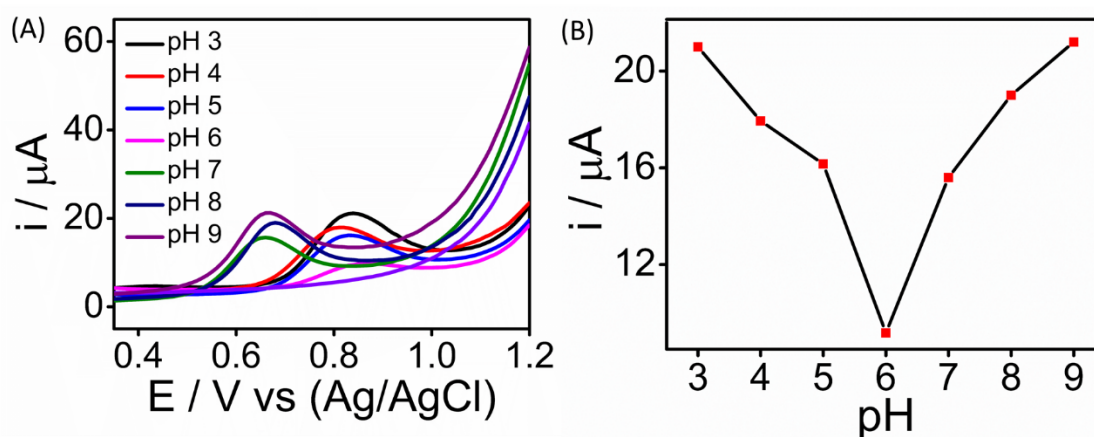


**Fig. S12.** (A) SWV of 5  $\mu$ M MTX in PBS buffer with pH values from 3 to 9 at SPCE/PrGO-PPy-Au, using optimized parameters: potential range 0.3V to 1.2V, frequency 10Hz, and amplitude 50mV. (B) The plot of peak potential and peak current vs. pH.

## 18. Selectivity

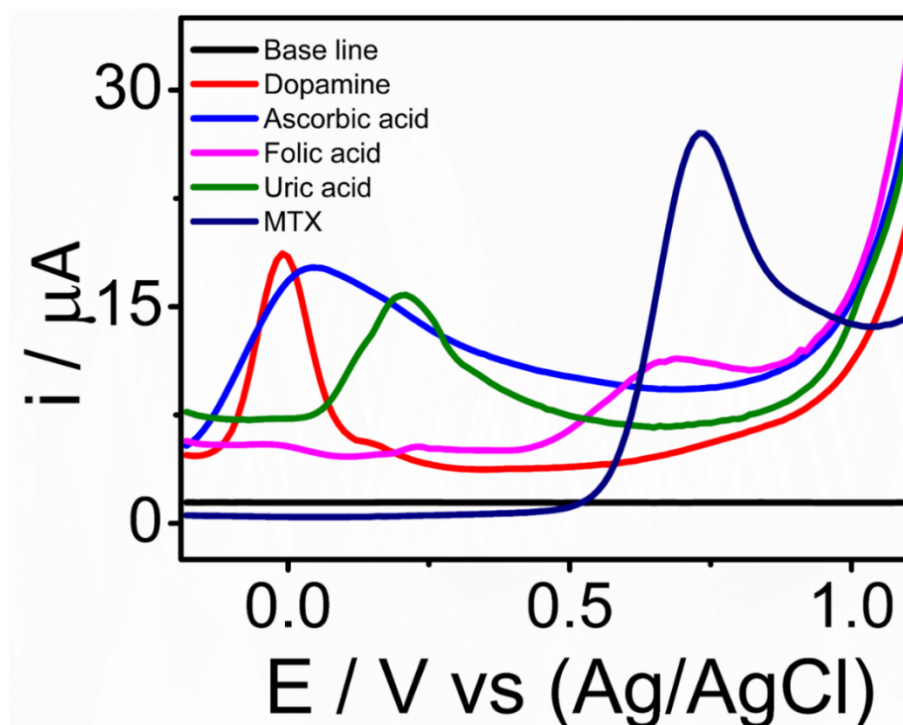


**Fig 13.** SWV response of the PrGO-PPy-Au sensor for methotrexate (MTX, 2  $\mu$ M) and interfering compounds including ascorbic acid (AA), folic acid (FA), uric acid (UA), and dopamine (DA), each at a concentration of 10  $\mu$ M.

## SUPPLEMENTARY INFORMATION

### 19. Comparison Table

**Table S2.** Comparison of the electroanalytical performance of the current modified sensor with existing literature.

Method	Electrodes	Medium	LOD	Reference
Electrochemical	SPCE/PrGO– PPy - Au	Human serum	0.4 nM	This work
Electrochemical	NHNC/GCE	PBS	10 nM	3
Electrochemical	f-CNTPE	Serum	2.9 nM	4
Electrochemical	GCE/NiO	Plasma	7.2 nM	5
Electrochemical	GCE/GO	Human serum	7.6 nM	6
Electrochemical	MIP/MWCNT/GCE	PBS	2.7 nM	7
Electrochemical	AuNPs CPE	Plasma	150 $\mu$ M	8
Electrochemical	GCE/GQD/AuNPs	Plasma	30 $\mu$ M	9

### 20. The detection limit (LOD) was calculated using the 3-sigma method

LOD =  $3 \times \frac{\text{Standard deviation}}{\text{Slope (SWV using Serum)}}$

Where:

- The Standard Deviation (SD) was calculated from the blank signal, which was 0.001.
- The Slope of the calibration curve, obtained from the linear regression of the concentration vs. current, was 6.311.

## SUPPLEMENTARY INFORMATION

Substituting these values into the formula

This resulted in a LOD of 0.4 nM.

### **21. Instrumentation**

In this research, screen-printed carbon electrodes (SPCEs) were produced using the MMP-SPM printer, a semi-automatic screen printing machine from Speedline Technologies. The working and counter electrodes were fabricated from graphite, offering both a large surface area and excellent conductivity. The Ag/AgCl pseudo reference electrode was selected for its stable and reproducible potential. SPCEs were created by depositing the electrode materials onto a flexible, disposable substrate using the screen-printing method. Electroanalytical measurements were performed at ambient temperature (25 °C) using an Emstat3 blue hand-held potentiostat from Palmsens B.V. The morphology of the hybrid nanocomposite was extensively examined using field emission scanning electron microscopy (FESEM) with a Gemini SEM300 instrument from Carl Zeiss AG. Prior to imaging, the sensor surface was sputtered with an Au/Pd layer, and imaging was carried out at an accelerating voltage of 10 kV and a pressure of 0.10 milliPascal to optimize the conditions. For chemical composition analysis, energy-dispersive X-ray spectroscopy (EDS) was conducted in conjunction with SEM. Raman spectroscopy measurements were taken with a Horiba Labram H Evo spectrophotometer from HORIBA France SAS. The Raman shifts were recorded from 500  $\text{cm}^{-1}$  to 5000  $\text{cm}^{-1}$  with a resolution of 0.5  $\text{cm}^{-1}$ , providing detailed spectral data. X-ray diffraction (XRD) spectra were acquired using a Smart Lab XR instrument from Rigaku Corporation, equipped with Cu  $K\alpha$  radiation ( $\lambda = 0.154 \text{ nm}$ ), and operated at 45 kV. Characterization was performed up to 1500°C, with measurements taken across a  $2\theta$  range of 10° - 100°, a step size of 0.02°, and a measurement time of 0.3 s per step to achieve high-resolution diffraction patterns. Additionally, the Horiba Labram HR Evo Raman spectrophotometer, capable of detecting absorption from 10 to 5000  $\text{cm}^{-1}$  with a resolution of 0.5  $\text{cm}^{-1}$  or better, was utilized. The X-ray photoelectron spectrometer (SPECS, Germany) was used to examine the material's composition, empirical formula, and element electronic states in the modified electrode. XPS spectra were obtained using Al  $K\alpha$  radiation (1486.6 eV) at 50 W, plotting kinetic energy or binding energy of electrons against electron intensity.



## SUPPLEMENTARY INFORMATION

### 22. References

- (1) Zaaba, N. I.; Foo, K. L.; Hashim, U.; Tan, S. J.; Liu, W.-W.; Voon, C. H. Synthesis of Graphene Oxide Using Modified Hummers Method: Solvent Influence. *Procedia Engineering* **2017**, *184*, 469–477. <https://doi.org/10.1016/j.proeng.2017.04.118>.
- (2) Budd, P. M.; Makhseed, S. M.; Ghanem, B. S.; Msayib, K. J.; Tattershall, C. E.; McKeown, N. B. Microporous Polymeric Materials. *Materials Today* **2004**, *7* (4), 40–46. [https://doi.org/10.1016/S1369-7021\(04\)00188-9](https://doi.org/10.1016/S1369-7021(04)00188-9).
- (3) Li, J.; Chen, D.; Zhang, T.; Chen, G. Highly Sensitive Electrochemical Determination of Methotrexate Based on a N-Doped Hollow Nanocarbon Sphere Modified Electrode. *Anal. Methods* **2021**, *13* (1), 117–123. <https://doi.org/10.1039/D0AY01996H>.
- (4) Kummari, S.; Kumar, V. S.; Satyanarayana, M.; Gobi, K. V. Direct Electrochemical Determination of Methotrexate Using Functionalized Carbon Nanotube Paste Electrode as Biosensor for In-Vitro Analysis of Urine and Dilute Serum Samples. *Microchemical Journal* **2019**, *148*, 626–633. <https://doi.org/10.1016/j.microc.2019.05.054>.
- (5) Zarean Mousabadi, K.; Ensafi, A. A.; Rezaei, B. Electrochemical Sensor for the Determination of Methotrexate Based on MOF-Derived NiO/Ni@C-Poly(Isonicotinic Acid). *Ind. Eng. Chem. Res.* **2023**, *62* (11), 4603–4610. <https://doi.org/10.1021/acs.iecr.2c03091>.
- (6) Chen, J.; Fu, B.; Liu, T.; Yan, Z.; Li, K. A Graphene Oxide-DNA Electrochemical Sensor Based on Glassy Carbon Electrode for Sensitive Determination of Methotrexate. *Electroanalysis* **2018**, *30* (2), 288–295. <https://doi.org/10.1002/elan.201700615>.
- (7) Jara-Cornejo, E.; Khan, S.; Vega-Chacón, J.; Wong, A.; Da Silva Neres, L. C.; Picasso, G.; Sotomayor, M. D. P. T. Biomimetic Material for Quantification of Methotrexate Using Sensor Based on Molecularly Imprinted Polypyrrole Film and MWCNT/GCE. *Biomimetics* **2023**, *8* (1), 77. <https://doi.org/10.3390/biomimetics8010077>.
- (8) Mir, A.; Shabani-Nooshabadi, M.; Ziaie, N. Determination of Methotrexate in Plasma and Environmental Samples Using an Electrochemical Sensor Modified by UiO66-NH<sub>2</sub>/Mesoporous Carbon Nitride Composite and Synergistic Signal Amplification with Decorated AuNPs. *Chemosphere* **2023**, *338*, 139427. <https://doi.org/10.1016/j.chemosphere.2023.139427>.
- (9) Zamani, M.; Tavakkoli, N.; Soltani, N. Electrochemical Sensor Based on Graphene Quantum Dot/Gold Nanoparticles and Thiol-Containing Organic Compound for Measuring Methotrexate Anti-Cancer Drug. *Diamond and Related Materials* **2023**, *136*, 109954. <https://doi.org/10.1016/j.diamond.2023.109954>.

**SUPPLEMENTARY INFORMATION**